

Recoil-distance lifetime measurements in $^{96,97,98}\text{Ru}$: Search for possible onset of collectivity at $N \geq 52$

B. Kharraja,* U. Garg, S. S. Ghugre,† and H. Jin

Department of Physics, University of Notre Dame, Notre Dame, Indiana 46556

R. V. F. Janssens, I. Ahmad, H. Amro, M. P. Carpenter, S. Fischer,‡ T. L. Khoo, T. Lauritsen, and D. Nisius§
Physics Division, Argonne National Laboratory, Argonne, Illinois 60439

W. Reviol, W. F. Mueller,|| and L. L. Riedinger

Department of Physics, University of Tennessee, Knoxville, Tennessee 37996

R. Kaczarowski and E. Ruchowska

Soltan Institute for Nuclear Studies, 05-400 Swierk, Poland

W. C. Ma

Department of Physics, Mississippi State University, Mississippi State, Mississippi 39762

I. M. Govil

Department of Physics, Panjab University, Chandigarh 160 014, India

(Received 28 April 1999; published 22 December 1999)

Lifetimes of high-spin states in the $N=52-54$ Ru nuclei have been investigated via the $^{65}\text{Cu}(^{36}\text{S},pyn)^{96,97,98}\text{Ru}$ ($\gamma=4,3,2$) reactions using the recoil-distance Doppler-shift technique. The data were collected in coincidence mode. Lifetimes have been extracted for both the positive- and the negative-parity states in ^{96}Ru and ^{98}Ru and for the positive-parity states in ^{97}Ru . The levels studied have lifetimes in the range 2–31 ps. The observed reduced transition probabilities $B(E2)$ and $B(M1)$ are compared with the predictions of the shell model. Theoretical implications of these results are discussed.

PACS number(s): 27.60.+j, 23.20.Lv, 21.60.Cs, 21.10.Tg

I. INTRODUCTION

The level structures of nuclei with $N \geq 50$ and $Z \geq 40$ exhibit an interesting interplay between single-particle and collective degrees of freedom. Nuclei with $N \leq 51$ are characterized by single-particle behavior [1], and collectivity dominates the excitation spectrum of heavier nuclei with $N \geq 55$ [2]. In order to understand the mechanisms responsible for the generation of high-spin states, to search for the possible onset of collectivity, and to delineate the transition from single-particle to collective behavior, we have recently performed extensive investigations of the $51 \leq N \leq 54$ nuclei $^{94,95}\text{Mo}$ [3], $^{94-96}\text{Tc}$ [4], $^{96-98}\text{Ru}$ [5], and $^{97,98}\text{Rh}$ [6]. In particular, extensive level schemes have been established for $^{96,97,98}\text{Ru}$ from data obtained with the early implementation phase of the Gammasphere array. The level structures of

these nuclei have been extended to rather high spins and excitation energies (for example, $I \approx 38\hbar$, $E_x \approx 23$ MeV in ^{98}Ru) [5]. The excitation energies, spins, and parities of most of the observed levels have been understood within the framework of the spherical shell model. In general, the observed structures of these nuclei were found to exhibit single-particle character even at the highest spins and excitation energies. The observation of γ rays with $E_\gamma \approx 2$ MeV, and the associated fragmentation of the γ -ray flux into many competing pathways, provided a clear experimental signature for the breaking of the $N=50$ core. This core-breaking picture is also supported qualitatively by the shell-model calculations and by the weak-coupling scheme [3].

On the other hand, theoretical calculations have predicted γ softness and shape coexistence persisting to high spins in these nuclei. Specifically, total Routhian surface (TRS) calculations of Wyss *et al.* [7] suggest the existence of deformed neutron configurations with negative parity based on the $\nu h_{11/2}$ neutron orbital in $^{96-98}\text{Ru}$. These can lead to a deformed minimum when aligned $g_{9/2}$ protons are added to the configuration. The resulting proton-neutron configurations would correspond to a near-prolate shape ($\gamma \sim 0^\circ$); however, the expected deformations are quite small ($\beta_2 < 0.13$) and the local minima in the TRS's rather shallow [8]. Experimentally, sequences of consecutive $E2$ transitions, with level spacings increasing with spin, have been observed in these nuclei [5,8]. These $E2$ transitions provided

*On leave from Physics Department, University Chouaib Doukali, BP 20, El Jadida, Morocco.

†Present address: IUCDAEF-Calcutta Center, Sector III/LB-8, Bidhan Nagar, Calcutta 700 091, India.

‡Present address: Physics Department, De Paul University, Chicago, IL 60614.

§Present address: Bio-Imaging Research Inc., Lincolnshire, IL 60069.

||Present address: NSCL, Michigan State University, East Lansing, MI 48824.

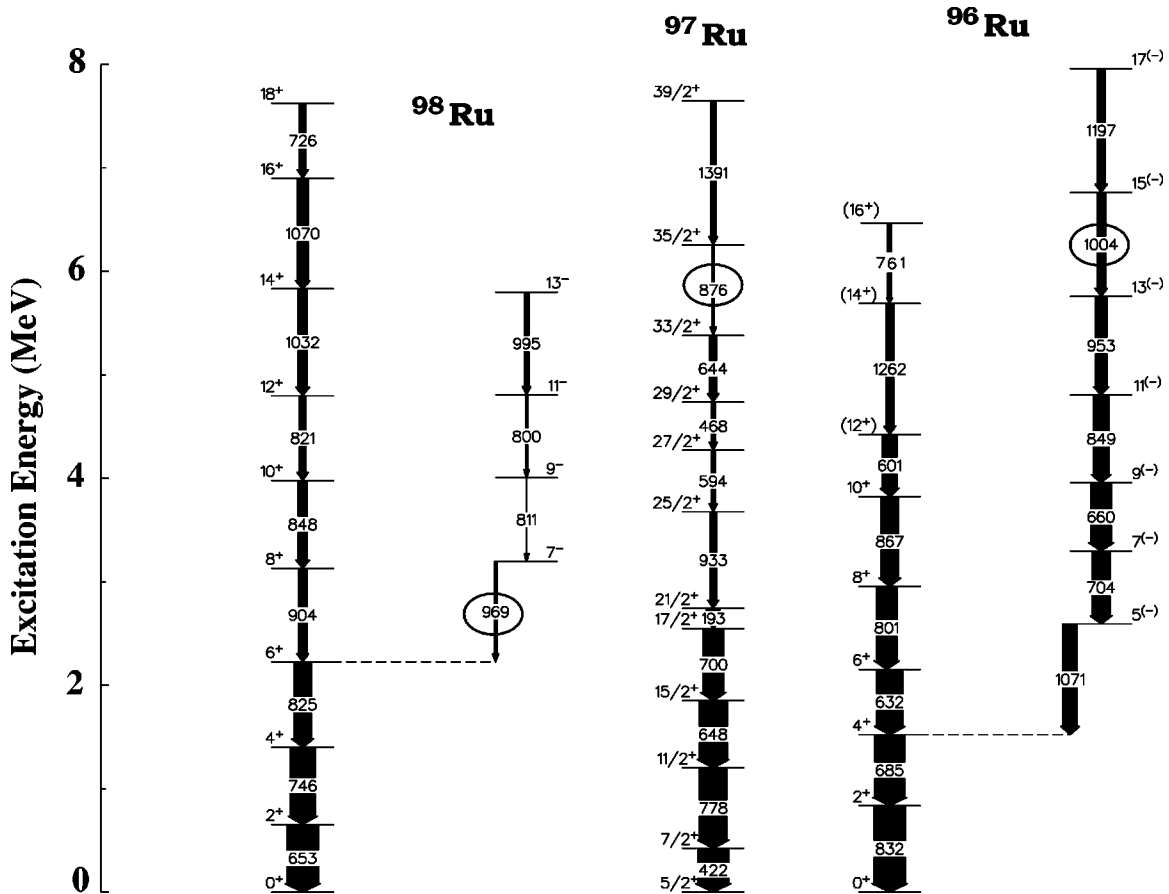


FIG. 1. Partial level schemes of ^{96}Ru , ^{97}Ru , and ^{98}Ru , showing only the transitions for which lifetimes could be measured. Some transitions (enclosed in ellipses) are included for the purpose of showing the complete decay sequence even though the corresponding lifetimes could not be measured. The energies are labeled in keV.

the first possible indications of the onset of collectivity for neutron numbers as low as $N=52$. However, it was found that the shell model can account for these $E2$ sequences reasonably well [5]. Thus, the true nature (collective or single-particle) of these $E2$ transitions has remained a subject of discussion.

The transition probabilities and the transition quadrupole moments extracted from experimental lifetime measurements are very valuable fingerprints of intrinsic single-particle configurations and can shed light on the true microscopic structure of the observed levels. Lifetime measurements, therefore, are critical to clarifying the ambiguity (single-particle or collective) presented by these “bandlike” $E2$ cascades. This was the main motivation behind the lifetime measurements in $^{96-98}\text{Ru}$ reported here.

II. EXPERIMENTAL PROCEDURE

The experiment was carried out with a 142 MeV ^{36}S beam obtained from the Argonne Tandem Superconducting Linear Accelerator System (ATLAS). This beam energy was found to optimize the yield of the pyn ($y=2,3,4$) reaction channels and resulted in an average velocity of $\beta \sim 3.26\%$ for the recoiling nuclei. A stretched, self-supporting,

1 mg/cm² thick, ^{65}Cu target foil was used and γ rays were detected with the Argonne-Notre Dame BGO γ -ray facility, consisting of 12 Compton-suppressed Ge detectors (25% nominal efficiency), four at each of the following angles: 34.5°, 90°, and 145.5° with respect to the beam direction, and a 50-element BGO inner array (used as a multiplicity filter). The Notre Dame plunger device was employed for the measurements wherein the stretched target foil could be moved by three computer-controlled dc actuators, allowing for a good accuracy in the positioning with respect to the stopper foil (a stretched, self-supporting, Au foil of 10 mg/cm² thickness), which was kept at a fixed position. The distance between the target and stopper foils was determined from the measured positions of the actuators and confirmed by measuring the capacitance between the two foils. The capacitance measurements were carried out before, during, and after the beam was on the target.

Because of the fragmentation of the total reaction strength among a number of competing reaction channels ($^{94-96}\text{Tc}$, $^{94,95}\text{Mo}$, $^{96-98}\text{Ru}$, and $^{97,98}\text{Rh}$) and the concomitant complexity of the observed spectra, data were collected in coincidence mode at 12 distances from 10 to 1010 μm , resulting in an effective lifetime range of ~ 1 –400 ps. A data set of approximately 165 million events was recorded,

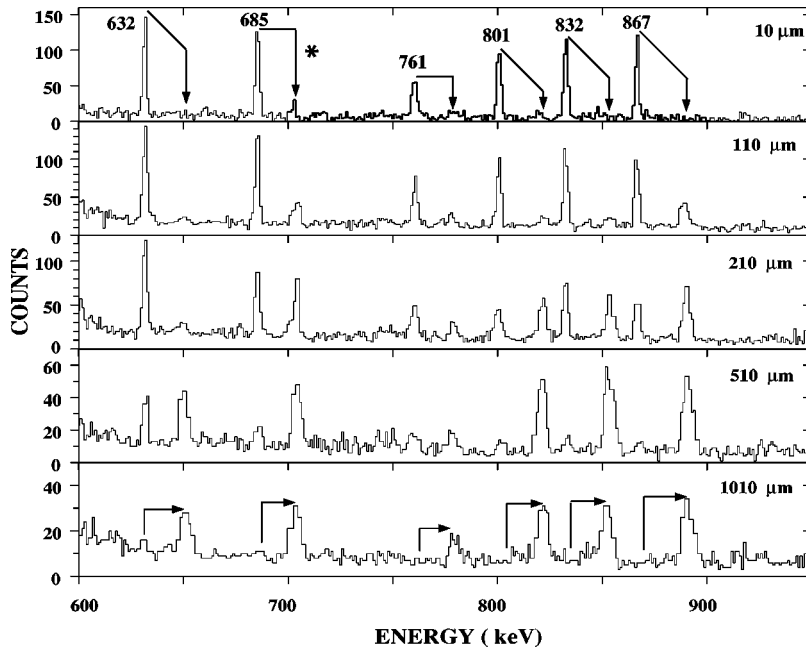


FIG. 2. Representative double-gated γ -ray coincidence spectra at the forward angle 34.5° for ^{96}Ru at the indicated distances. The 703-keV transition, indicated by an asterisk in the uppermost panel, is a contaminant (see text).

requiring a prompt coincidence between two Compton-suppressed Ge's and at least two BGO-array elements.

III. DATA ANALYSIS

The areas of the shifted (in flight) and unshifted (stopped) components of the γ -ray transitions were extracted from the gated coincidence spectra. The relative intensities for the observed states were determined from the data collected at 90° . Lifetimes were deduced in the usual manner from the distance dependence of the ratios R_d , of the intensity of the unshifted component to the sum of the shifted and unshifted intensities, using the computer code LIFETIME [9]. Each set of R_d ratios defined a curve for a given transition and the lifetimes of levels, as well as those of the corresponding feeding transitions, were extracted from fits to these R_d curves. In extracting lifetime information, LIFETIME takes into account corrections due to side feeding, changes in the solid angle due to the changing position of the recoiling nucleus along the flight path, velocity transformation of the solid angle due to the relativistic motion of the ion, changes in the angular distribution due to the attenuation of alignment during recoil, changes in intensities due to the slowing of the recoil nucleus in the stopper, detector efficiency, and internal conversion. In general, the most significant correction results from the effects of the feeding of the levels under investigation: one component of the feeding originates from the next higher transition in the cascade under study, while the other represents all other unobserved feeding transitions (side feeding). In our measurements, for most of the transitions under investigation, it was possible to place coincidence gates on the “higher” in-band transitions feeding the level under consideration, thus avoiding any contribution from the side feeding. In some cases, where limited statistics did not permit clean gates on higher transitions, the lifetime of the side feeding transitions was treated as a free parameter in the fitting process. Also, to minimize the errors on each lifetime,

the data for the highest transition were fitted first and the data for transitions lower down in the cascade were added in each successive step. The roughness of the target and/or stopper surface also affects the value of R_d for a given distance d and therefore, the extracted lifetimes. This effect, although small in our measurements, can be taken into account in the fitting procedure, to a very good approximation, by treating the smallest distance d_0 as a free parameter and adjusting the other distances accordingly.

IV. EXPERIMENTAL RESULTS

Figure 1 presents partial level schemes of $^{96-98}\text{Ru}$ showing all the transitions for which reliable lifetime information was extracted in the present investigation. Sample spectra for several target-stopper distances, taken with the detectors placed at 34.5° , are shown in Fig. 2, with the corresponding target-stopper distance given in the upper right corner of each spectrum. These spectra were obtained by setting gates on the 601 keV, $12^+ \rightarrow 10^+$ transition in ^{96}Ru . Although this transition is actually a triplet, it was still possible to obtain good-quality gated spectra, as Fig. 2 shows. The transitions of interest are labeled and the positions of the Doppler-shifted and unshifted peaks are marked. The presence of a 703 keV γ ray in the spectra for $d=10 \mu\text{m}$ needs to be addressed. This transition has the same energy as the forward-shifted component of the 685 keV γ ray and appears in the spectrum because it is in coincidence with another 601-keV line (connecting the 21^- and 19^- levels). However, because the 666-keV, backward-shifted component of the 685 keV γ ray, is not present at 135.5° , it may be safely assumed that all of the intensity of the 703 keV γ ray at $10 \mu\text{m}$ is due to contamination.

The nucleus ^{96}Ru has three transitions (two of $E2$ and one of $E1$ character) with rather close energies (~ 1000 keV) [5]. These transitions belong to the negative-parity sequence and are in coincidence with each other. Fur-

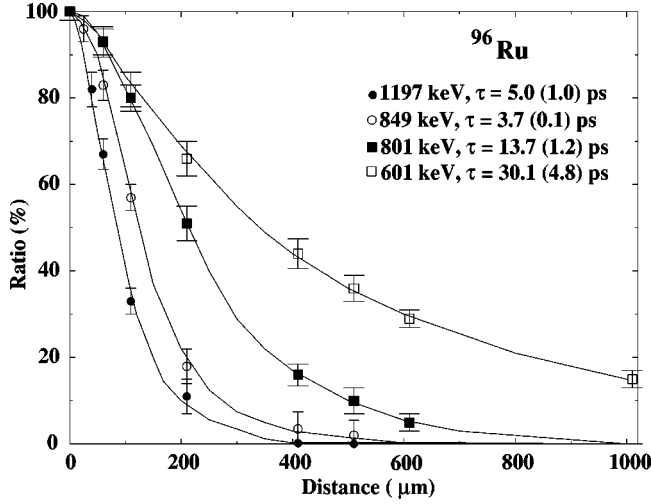


FIG. 3. Examples of fits to the ratios R_d (as defined in the text), of γ -ray transitions in both the positive- and negative-parity cascades in ^{96}Ru , as a function of the separation between target and stopper d .

thermore, the shifted component of this ‘‘composite transition’’ at forward angles is contaminated by other γ lines from ^{98}Ru . Due to these constraints, no reliable lifetime information could be extracted for these transitions. However, it was possible to obtain an upper limit for the lifetime of the $17^{(-)}$ level. In all, lifetimes were extracted for ^{96}Ru up to $14^{(+)}$ in the positive-parity sequence, and up to $13^{(-)}$ in the negative-parity sequence, using a number of different gated spectra. Typical fits of the data for both positive- and negative-parity sequences are illustrated in Fig. 3, and the corresponding lifetimes are summarized in Table I. The only previously reported lifetimes (as compiled in ENSDF) relevant to the present work are for the 2^+ and 4^+ states (4.1 ± 0.2 ps and 10.1 ± 1.3 ps, respectively) and our results are in agreement with those.

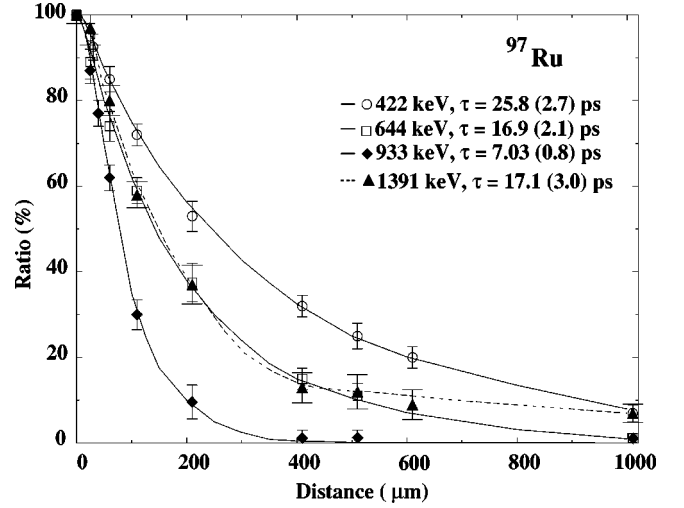


FIG. 4. Examples of fits to the ratios R_d (as defined in the text), of γ -ray transitions in the positive-parity cascade in ^{97}Ru , as a function of the separation between target and stopper, d .

In contrast with ^{96}Ru and ^{98}Ru , the negative-parity sequence observed in ^{97}Ru is very weakly populated [5]; therefore, no lifetimes could be obtained for this sequence. However, lifetimes have been extracted for the transitions in the positive-parity band, decaying from the $33/2^+$ level to the ground state; the lifetime for the $35/2^+$ level could not be extracted because of the weak intensity of the 876 keV ($35/2^+ \rightarrow 33/2^+$) γ ray. The present data indicate decreasing values of τ , from 25.8 ps for the $7/2^+$ level to 7.0 ps for the $25/2^+$ level, then increasing up to 17.1 ps for the 1391 keV γ -ray transition. Representative fits for the R_d curves of the 422, 644, 933, and 1391 keV transitions are shown in Fig. 4; the extracted lifetimes are listed in Table II. Comparison with the compiled lifetime data (in ENSDF) indicates a rather poor agreement for the 422-keV ($7/2^+ \rightarrow 5/2^+$) transition;

TABLE I. Energies, spins, relative intensities, lifetimes, and comparison between the experimental and theoretical $B(E2)$ values for levels up to $J=(16^+)$ and $17^{(-)}$ in ^{96}Ru .

E_γ (keV)	$J_i \rightarrow J_f$ \hbar	I_γ %	τ (ps)	$B(E2)_{\text{expt}}$ $10^{-3} e^2 b^2$	$B(E2)_{\text{SM}}$ $10^{-3} e^2 b^2$	$B(E2)_{\text{expt}}$ (W.u.) ^a	$B(E2)_{\text{SM}}$ (W.u.) ^a
832	$2^+ \rightarrow 0^+$	100.0	5.1 ± 0.5	40.1 ± 3.9	41.46	15.30 ± 1.5	15.8
685	$4^+ \rightarrow 2^+$	94.1	9.8 ± 1.0	55.3 ± 5.6	52.72	21.6 ± 2.1	20.1
632	$6^+ \rightarrow 4^+$	82.8	18.3 ± 1.4	44.2 ± 4.5	39.38	16.9 ± 1.7	15.0
801	$8^+ \rightarrow 6^+$	64.1	13.7 ± 1.2	18.0 ± 2.0	20.72	6.87 ± 0.8	7.91
867	$10^+ \rightarrow 8^+$	55.1	5.1 ± 0.5	32.64 ± 3.2	39.5	12.5 ± 1.2	15.1
601	$(12^+) \rightarrow 10^+$	12.5	30.9 ± 4.8	33.66 ± 5.2	34.44	12.8 ± 2.0	13.2
1262	$(14^+) \rightarrow (12^+)$	22.7	3.5 ± 0.3	6.87 ± 1.0	31.53	2.63 ± 0.4	12.0
761	$(16^+) \rightarrow (14^+)$	10.3	≤ 10.7	≥ 38.8	13.1	≥ 14.8	5.0
704	$7^{(-)} \rightarrow 5^{(-)}$	55.1	10.2 ± 1.3	46.2 ± 5.9	49.41	17.6 ± 2.3	18.9
660	$9^{(-)} \rightarrow 7^{(-)}$	61.1	12.0 ± 1.2	54.3 ± 5.4	62.12	20.7 ± 2.1	23.7
849	$11^{(-)} \rightarrow 9^{(-)}$	51.3	3.7 ± 0.7	50.0 ± 9.5	53.1	19.1 ± 3.6	20.3
953	$13^{(-)} \rightarrow 11^{(-)}$	38.2	3.1 ± 0.6	33.5 ± 6.4	45.15	12.6 ± 2.4	17.2
1004	$15^{(-)} \rightarrow 13^{(-)}$	24.2			35.05		13.38
1197	$17^{(-)} \rightarrow 15^{(-)}$	24.1	≤ 6.0	≥ 8.0	24.58	≥ 3.0	9.36

^a1 Weisskopf unit (W.u.) = $2.62 \times 10^{-3} e^2 b^2$.

TABLE II. Energies, spins, relative intensities, lifetimes, and comparison between the experimental and theoretical $B(E2)$ values for levels up to $J=39/2^+$ in ^{97}Ru .

E_γ (keV)	$J_i \rightarrow J_f$ \hbar	I_γ %	τ (ps)	$B(M1)_{\text{expt}}$ $10^{-3} \mu_N^2$	$B(M1)_{\text{SM}}$ $10^{-3} \mu_N^2$	$B(M1)_{\text{expt}}$ 10^{-3} (W.u.) ^a	$B(M1)_{\text{SM}}$ 10^{-3} (W.u.) ^a
422 ^a	$7/2^+ \rightarrow 5/2^+$	100	25.8 ± 2.7	29.4 ± 3.1	43.1	16.4 ± 1.7	24.1
700 ^a	$17/2^+ \rightarrow 15/2^+$	71.0	16.4 ± 1.8	10.1 ± 1.1	9.0	5.7 ± 0.6	5.0
594 ^a	$27/2^+ \rightarrow 25/2^+$	15.3	7.1 ± 0.9	38.3 ± 4.9	15.2	21.3 ± 2.7	8.5
468 ^a	$29/2^+ \rightarrow 27/2^+$	14.7	10.2 ± 1.3	30.8 ± 3.9	37.0	17.2 ± 2.2	20.7
E_γ (keV)	$J_i \rightarrow J_f$ \hbar	I_γ %	τ (ps)	$B(E2)_{\text{expt}}$ $10^{-3} e^2 b^2$	$B(E2)_{\text{SM}}$ $10^{-3} e^2 b^2$	$B(E2)_{\text{expt}}$ (W.u.) ^b	$B(E2)_{\text{SM}}$ (W.u.) ^b
778 ^b	$11/2^+ \rightarrow 7/2^+$	86.1	15.1 ± 2.3	16.07 ± 2.4	7.1	6.05 ± 0.9	2.67
648 ^b	$15/2^+ \rightarrow 11/2^+$	87.2	16.7 ± 2.3	42.8 ± 5.9	31.0	16.12 ± 2.2	11.67
193 ^b	$21/2^+ \rightarrow 17/2^+$	37.7	10.6 ± 1.2	0.25 ± 0.03	0.210	0.14 ± 0.01	0.117
933 ^b	$25/2^+ \rightarrow 21/2^+$	20.1	7.0 ± 0.8	16.4 ± 1.9	14.4	6.18 ± 0.7	5.42
644 ^b	$33/2^+ \rightarrow 29/2^+$	20.7	≤ 18.0	≥ 38.8	21.7	≥ 14.6	8.17
1391 ^b	$39/2^+ \rightarrow 35/2^+$	14.2	≤ 20.1	≥ 0.92	4.21	≥ 0.40	1.58

^aFor these $M1$ transitions, 1 Weisskopf unit = $1.791 \mu_N^2$.

^bFor these $E2$ transitions, 1 Weisskopf unit (W.u.) = $2.65 \times 10^{-3} e^2 b^2$.

the reasons for this lack of agreement in this one case are not readily apparent.

It was possible to extract lifetimes for the levels below spin $18\hbar$ in the positive-parity sequence (states between 2^+ and 18^+) in ^{98}Ru . In this case, the forward-shifted component of the 825 keV transition ($6^+ \rightarrow 4^+$) could not be resolved from the 848 keV transition feeding the 8^+ level. Therefore, the shifted component in the backward detectors was used to extract the lifetime of the 6^+ level. Although, the backward component has an energy of 801 keV, close to the energy of the transition feeding the 9^- state, it was easy to resolve this problem by obtaining spectra gated by transitions above the 6^+ level. On the other hand, to minimize the contribution from the contaminant transitions, only the unshifted component was used to obtain a lifetime for the 821 keV transition feeding the 10^+ state. Because the statistics in

the spectra obtained by setting coincidence gates above the 14^+ level was rather poor, the spectra used to extract lifetimes of the 1032, 1070, and 726 keV transitions were obtained by using gates below the 10^+ level. In these cases, as described earlier, the side-feeding effects were accounted for by assuming a single lifetime associated with all unobserved feeding and treating it as a variable parameter in the fits. The side feeding time corresponding to these transitions is also shown in Table III.

Due to lack of sufficient statistics, lifetimes in the negative-parity sequence have been extracted only for states below the 13^- level. Decay curves of the 653, 811, 995, and 1070 keV transitions are presented in Fig. 5 and Table III summarizes the transition energies, spins, and measured lifetimes for γ rays belonging to ^{98}Ru . A comparison with the previously-reported lifetimes indicates very good agreement

TABLE III. Energies, spins, relative intensities, lifetimes, side feeding times, and comparison between the experimental and theoretical $B(E2)$ values for levels up to $J=18^+$ and 13^- in ^{98}Ru .

E_γ (keV)	$J_i \rightarrow J_f$ \hbar	I_γ %	τ (ps)	τ_{sf} (ps)	$B(E2)_{\text{expt}}$ $10^{-3} e^2 b^2$	$B(E2)_{\text{SM}}$ $10^{-3} e^2 b^2$	$B(E2)_{\text{expt}}$ (W.u.) ^a	$B(E2)_{\text{SM}}$ (W.u.) ^a
653	$2^+ \rightarrow 0^+$	100	8.0 ± 1.2		85.8 ± 12.9	41.35	31.9 ± 4.8	15.37
746	$4^+ \rightarrow 2^+$	78.4	11.0 ± 2.3		32.1 ± 6.7	35.22	11.9 ± 2.5	13.1
825	$6^+ \rightarrow 4^+$	59.1	6.2 ± 0.7		34.70 ± 3.9	28.39	12.9 ± 1.5	10.6
904	$8^+ \rightarrow 6^+$	24.3	20.1 ± 3.0		6.72 ± 1.0	12.79	2.51 ± 0.4	4.75
848	$10^+ \rightarrow 8^+$	28.4	6.6 ± 0.5		28.18 ± 2.1	41.45	10.5 ± 0.8	15.4
821	$12^+ \rightarrow 10^+$	24.3	9.3 ± 0.7		23.5 ± 1.8	5.86	8.71 ± 0.7	2.18
1032	$14^+ \rightarrow 12^+$	31.5	2.1 ± 0.2	0.5	34.00 ± 3.2	26.82	12.6 ± 1.2	9.97
1070	$16^+ \rightarrow 14^+$	32.2	4.5 ± 1.1	1.0	13.0 ± 3.2	87.14	4.82 ± 1.2	32.4
726	$18^+ \rightarrow 16^+$	24.5	≤ 8.7		≥ 59.0		≥ 22.0	
811	$9^- \rightarrow 7^-$	3.2	20.6 ± 3.0		11.3 ± 1.6	9.1	4.2 ± 0.6	3.38
800	$11^- \rightarrow 9^-$	6.3	4.1 ± 0.4		60.71 ± 6.2	54.53	22.5 ± 2.3	20.3
995	$13^- \rightarrow 11^-$	12.2	≤ 2.3		≥ 43.6	44.97	≥ 16.2	16.7

^a1 Weisskopf unit (W.u.) = $2.69 \times 10^{-3} e^2 b^2$.

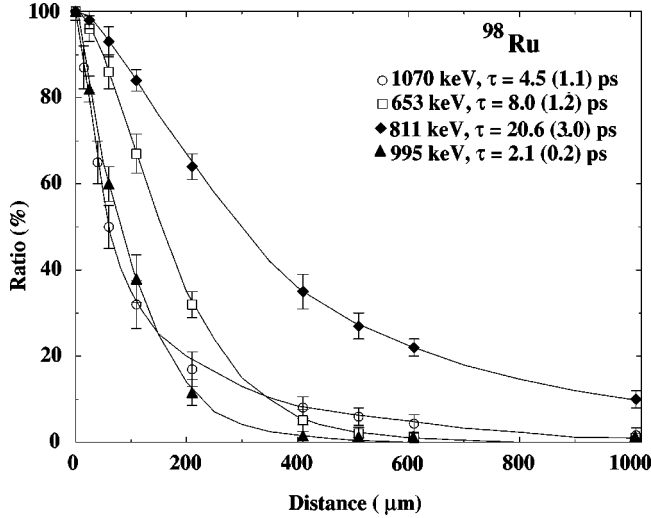


FIG. 5. Examples of fits to the ratios R_d (as defined in the text), of γ -ray transitions in both the positive- and negative-parity cascades in ^{98}Ru , as a function of the separation between target and stopper d .

for the 2^+ state (ENSDEF value 8.8 ± 0.3 ps), but a significant difference for the 4^+ state (ENSDEF value 3.3 ± 0.8 ps); again, the reasons for this disagreement are not readily apparent.

In order to evaluate the effect of the sidefeeding on the extracted lifetimes, we have compared the lifetimes for the 632-keV, ($6^+ \rightarrow 4^+$) transition in ^{96}Ru , obtained with and without side feeding. In the first case, a coincidence gate was set below this transition and led to a value of $\tau_1 = 20.1(2.3)$ ps. This compares with $\tau_2 = 18.3(1.4)$ ps, obtained with gating on the high-lying transitions feeding the 6^+ state. Similar analyses have been performed for the 801-keV ($8^+ \rightarrow 6^+$) transition in ^{96}Ru , as well as for the 653- and 746-keV transitions in ^{98}Ru . In all cases, the difference between τ_1 and τ_2 is about 10% and falls within the error bars of the quoted numbers, thus establishing the veracity of the treatment of side feeding in our analyses.

V. DISCUSSION

The negative-parity sequence of ^{96}Ru includes quadrupole transitions with energies increasing with spin. The γ ray transitions in this cascade, observed between spins 7^- and 23^- , have respective energies of 660, 849, 953, 1004, 1197, 1440, and 1600 keV and may be constructed as forming a rotational band. However, as mentioned earlier, good agreement was obtained between the spherical shell model calculations and the experimental excitation energies, suggesting that invoking collectivity may not be necessary. A clear indication of the collective nature of these transitions would be provided by strongly enhanced $B(E2)$ transition probabilities in comparison with the Weisskopf estimates (W.U.). However, the experimental transition probabilities for the transitions in this sequence are all rather small (≤ 20 W.U.), thus establishing their non-collective origin.

We have compared the experimental $B(E2)$ values with theoretical predictions from spherical shell model calcula-

tions. The calculations were performed within the model space named GL in the code OXBASH [10]. This model space encompasses the $\pi(p_{1/2}, g_{9/2})$ and $\nu(d_{5/2}, s_{1/2})$ orbits outside the ^{88}Sr inert core. The two-body matrix elements were taken from the work of Gloeckner [11] and include no contribution from core excitation. Within the restricted model space used, the maximum angular momentum possible for ^{96}Ru , with six valence protons and two valence neutrons outside ^{88}Sr , is $J = 16\hbar$. Details of these calculations are provided in Refs. [5,12] and the results are summarized in Table I. As can be seen, there is a rather good agreement between the experimental transition probabilities and the shell-model estimates for ^{96}Ru up to spin 12^+ . This, in itself, is quite remarkable considering the very limited configuration space used in these calculations [5] and, affirms the validity of the two-body interactions employed. On the other hand, the calculated and experimental $B(E2)$'s are significantly different for the states above the 14^+ level [for example, for the 1262 keV transition, $B(E2)_{\text{SM}} \sim 5 \times B(E2)_{\text{exp}}$]. However, this discrepancy occurs near the spin where the breaking of the $N = 50$ core is observed [5] and the shell-model calculations become overly elaborate and complex. The shell model calculations also reproduce fairly well the experimental transition probabilities for the negative parity sequence up to spin 13^- .

It would appear, then, that although the aforementioned negative-parity cascade comprises a series of $E2$ transitions with energies increasing monotonically with the spin (akin to those in a collective rotational band), it, in fact, corresponds to a structure of single-particle nature. The states of the positive-parity cascade are, as expected, associated with single-particle excitations.

A similar comparison between the experimental $B(E2)$ and $B(M1)$ values and their shell-model counterparts for ^{97}Ru is presented in Table II. In general, there is again good agreement between the experimental and the calculated values especially for the $15/2^+$, $17/2^+$, $21/2^+$, and $27/2^+$ levels. However, the agreement between the calculated and measured transition probabilities is of a poor quality for the $5/2^+$, $7/2^+$, $11/2^+$, and $25/2^+$ levels. These also are levels whose energies were reproduced rather poorly by the shell-model calculations [5], thus indicating that the intrinsic configurations of these levels are quite different from those assumed in the calculations.

In Ref. [5] we have reported a $\Delta J = 2$ sequence built on the 11^- level in ^{97}Ru . Its energy spacing is similar to others observed in the $^{99,101}\text{Ru}$ nuclei [2]. However, in these heavier isotopes ($N = 55$ and 57), the negative-parity cascades are much stronger and are of collective nature, involving the $h_{11/2}$ orbital. Unfortunately, no lifetimes could be extracted for this cascade in the present work. Therefore, in light of our results, it is not possible to confirm or rule out about the onset of collectivity in the Ru nuclei at $N = 53$.

The level scheme of ^{98}Ru consists of two separate sequences of positive and negative parity with no interband transitions above spin 6^+ [5]. The positive-parity sequence shows transitions without any regular pattern, while the negative-parity sequence consists of states with a rather regular spacing and linked by $E2$ transitions of energies 800,

995, 1230, 1287, and 1404 keV, respectively, between the levels 9^- and 19^- . At first glance, this sequence also resembles a rotational band. However, in our previous work [5], we have presented a description of these levels in terms of spherical shell model calculations. Just as in ^{96}Ru , reasonable agreement was obtained between the theoretical and experimental values, up to the highest spins observed. Furthermore, in a previous attempt at understanding the nature of ^{98}Ru , IBA calculations were performed for the low-lying levels (up to spin 10^+), leading to the conclusion that ^{98}Ru can be described well by the IBA-1 model (in its vibrational limit) up to spin 8^+ , beyond which the experimental excitation energies deviate significantly from the calculated ones [13]. A different explanation for the structure of ^{98}Ru has been suggested by Samudra *et al.*, using the surface-delta residual interaction in a two-quasiparticle-plus rotor model [14]. Further, E2 transitions of almost equal energy (~ 2 MeV) are observed in this nucleus at high spin, beyond the value where ‘‘core breaking’’ occurs.

Table III shows a comparison of the experimental $B(E2)$ value for ^{98}Ru with those obtained using the shell model calculations. It is clear that the agreement between the theory and the experiment is less satisfactory for the positive-parity cascade than it is in the case of ^{96}Ru . In particular, the calculated $B(E2)$ of the $2^+ \rightarrow 0^+$ transition (653 keV) is only about half as much as that extracted from the measured lifetime of this level (which, as pointed out earlier, confirms the previously-measured lifetime of this transition [15]). On the other hand, there is good agreement between experiment and theory for the $B(E2)$ values in the negative-parity sequence.

VI. SUMMARY AND CONCLUSIONS

In summary, lifetimes have been measured with the recoil distance method for the low- and moderate-spin transitions

in $^{96,97,98}\text{Ru}$ in order to investigate in detail whether the observed E2 ‘‘bandlike’’ cascades in these nuclei are of collective nature. The results were compared with predictions of spherical shell model. The experimental transition probabilities were found to be in agreement with the shell-model calculations for ^{96}Ru up to spins where the onset of the $N = 50$ core breaking had been previously observed. Although extended calculations, taking into account all the configurations involved, are beyond the scope of this work, it is clear that single-particle excitations dominate the yrast and near-yrast structures in this nucleus. The positive parity states of ^{97}Ru are also associated with single-particle nature, in this case too, any better agreement between the theoretical and the experimental transition probabilities, would require more elaborate shell model calculations, involving specifically the $g_{7/2}$ orbital. The experimental data are not sufficient to draw any conclusions regarding the possible presence of collectivity in the negative-parity cascade of this nucleus. A qualitative agreement between the experimental transition probabilities and shell-model calculations has been obtained for ^{98}Ru as well. The measured transition probabilities in ^{98}Ru suggest that this nucleus is most likely characterized by both single-particle excitations and by a vibrationlike behavior.

ACKNOWLEDGMENTS

This work has been supported in part by the National Science Foundation (Grant No. PHY94-02761), the U.S. Department of Energy (Contract Nos. W-31-109-ENG-38 and DE-FG05-87ER40361) and the Polish-American Maria Sklodowska-Curie Joint Fund II (Project No. PPA/DOE-93-153).

-
- [1] S.S. Ghugre, S.B. Patel, M. Gupta, R.K. Bhowmik, and J.A. Sheikh, *Phys. Rev. C* **50**, 1346 (1994).
- [2] J. Gizon, D. Jerrestam, A. Gizon, M. Jozsa, R. Bark, B. Fogelberg, E. Ideguchi, W. Klamra, T. Lindblad, S. Mitarai, J. Nyberg, M. Piiparinen, and G. Sletten, *Z. Phys. A* **345**, 335 (1993).
- [3] B. Kharraja, S.S. Ghugre, U. Garg, R.V.F. Janssens, M.P. Carpenter, B. Crowell, T.L. Khoo, T. Lauritsen, D. Nisius, W. Reviol, W.F. Mueller, L.L. Riedinger, and R. Kaczarowski, *Phys. Rev. C* **57**, 2903 (1998).
- [4] S.S. Ghugre, B. Kharraja, U. Garg, R. V. F. Janssens, M. P. Carpenter, B. Crowell, T. L. Khoo, T. Lauritsen, D. Nisius, W. Reviol, W. F. Mueller, L. L. Riedinger, and R. Kaczarowski, *Phys. Rev. C* **61**, 024302 (1999).
- [5] B. Kharraja, S.S. Ghugre, U. Garg, M.P. Carpenter, B. Crowell, R.V.F. Janssens, T.L. Khoo, T. Lauritsen, D. Nisius, W.F. Mueller, W. Reviol, L.L. Riedinger, and R. Kaczarowski, *Phys. Rev. C* **57**, 83 (1998).
- [6] S.S. Ghugre, B. Kharraja, U. Garg, R.V.F. Janssens, M.P. Carpenter, B. Crowell, T.L. Khoo, T. Lauritsen, D. Nisius, W. Reviol, W.F. Mueller, L.L. Riedinger, and R. Kaczarowski, *Phys. Rev. C* **58**, 3243 (1998).
- [7] R. Wyss (private communication).
- [8] W. Reviol, U. Garg, A. Aprahamian, M.P. Carpenter, B.F. Davis, D. Ye, R.V.F. Janssens, T.L. Khoo, T. Lauritsen, Y. Liang, S. Naguleswaran, and J.C. Walpe, *Nucl. Phys.* **A557**, 391c (1993).
- [9] Computer code LIFETIME, obtained from J. C. Wells, Oak Ridge National Laboratory, Oak Ridge, Tennessee.
- [10] B.A. Brown, A. Etchegoyen, W.D.M. Rae, and N.S. Godwin, MSU-NSCL Report No. 524, 1985 (unpublished).
- [11] D.H. Gloeckner, *Nucl. Phys.* **A253**, 301 (1975).
- [12] S.S. Ghugre and S.K. Datta, *Phys. Rev. C* **52**, 1881 (1995).
- [13] E.H. Du Marchie Van Voorthuysen, M.J.A. DeVoigt, N. Blasi, and J.F.W. Jansen, *Nucl. Phys.* **A355**, 93 (1981).
- [14] G.S. Samudra, K.D. Carnes, F.A. Rickey, P.C. Simms, and S. Zeghib, *Phys. Rev. C* **37**, 605 (1988).
- [15] S. Raman, C.H. Malarkey, W. Milner, C.W. Nestor, Jr., and P.H. Stelson, *At. Data Nucl. Data Tables* **36**, 45 (1987), and references therein.